

---

---

# <sup>124</sup>I-MIBG PET/CT to Monitor Metastatic Disease in Children with Relapsed Neuroblastoma

Mariam S. Aboian<sup>1,2</sup>, Shih-ying Huang<sup>1</sup>, Miguel Hernandez-Pampaloni<sup>1</sup>, Randall A. Hawkins<sup>1</sup>, Henry F. VanBrocklin<sup>1</sup>, Yoonsuk Huh<sup>1</sup>, Kieuhoa T. Vo<sup>3</sup>, W. Clay Gustafson<sup>3</sup>, Katherine K. Matthay<sup>3</sup>, and Youngho Seo<sup>1,4</sup>

<sup>1</sup>Department of Radiology and Biomedical Imaging, University of California, San Francisco, San Francisco, California; <sup>2</sup>Department of Radiology and Biomedical Imaging, Yale University, New Haven, Connecticut; <sup>3</sup>Department of Pediatrics, University of California, San Francisco, San Francisco, California; and <sup>4</sup>Department of Radiation Oncology, University of California, San Francisco, San Francisco, California

---

The metaiodobenzylguanidine (MIBG) scan is one of the most sensitive noninvasive lesion detection modalities for neuroblastoma. Unlike <sup>123</sup>I-MIBG, <sup>124</sup>I-MIBG allows high-resolution PET. We evaluated <sup>124</sup>I-MIBG PET/CT for its diagnostic performance as directly compared with paired <sup>123</sup>I-MIBG scans. **Methods:** Before <sup>131</sup>I-MIBG therapy, standard <sup>123</sup>I-MIBG imaging (5.2 MBq/kg) was performed on 7 patients, including whole-body (anterior–posterior) planar imaging, focused-field-of-view SPECT/CT, and whole-body <sup>124</sup>I-MIBG PET/CT (1.05 MBq/kg). After therapy, 2 of 7 patients also completed <sup>124</sup>I-MIBG PET/CT as well as paired <sup>123</sup>I-MIBG planar imaging and SPECT/CT. One patient underwent <sup>124</sup>I-MIBG PET/CT only after therapy. We evaluated all 8 patients who showed at least 1 <sup>123</sup>I-MIBG–positive lesion with a total of 10 scans. In 8 pairs, <sup>123</sup>I-MIBG and <sup>124</sup>I-MIBG were performed within 1 mo of each other. The locations of identified lesions, the number of total lesions, and the curie scores were recorded for the <sup>123</sup>I-MIBG and <sup>124</sup>I-MIBG scans. Finally, for 5 patients who completed at least 3 PET/CT scans after administration of <sup>124</sup>I-MIBG, we estimated the effective dose of <sup>124</sup>I-MIBG. **Results:** <sup>123</sup>I-MIBG whole-body planar scans, focused-field-of-view SPECT/CT scans, and whole-body <sup>124</sup>I-MIBG PET scans found 25, 32, and 87 total lesions, respectively. There was a statistically significant difference in lesion detection for <sup>124</sup>I-MIBG PET/CT versus <sup>123</sup>I-MIBG planar imaging ( $P < 0.0001$ ) and <sup>123</sup>I-MIBG SPECT/CT ( $P < 0.0001$ ). The curie scores were also higher for <sup>124</sup>I-MIBG PET/CT than for <sup>123</sup>I-MIBG planar imaging and SPECT/CT in 6 of 10 patients. <sup>124</sup>I-MIBG PET/CT demonstrated better detection of lesions throughout the body, including the chest, spine, head and neck, and extremities. The effective dose estimated for patient-specific <sup>124</sup>I-MIBG was approximately 10 times that of <sup>123</sup>I-MIBG; however, given that we administered a very low activity of <sup>124</sup>I-MIBG (1.05 MBq/kg), the effective dose was only approximately twice that of <sup>123</sup>I-MIBG despite the large difference in half-lives (100 vs. 13.2 h). **Conclusion:** The first-in-humans use of low-dose <sup>124</sup>I-MIBG PET for monitoring disease burden demonstrated tumor detection capability superior to that of <sup>123</sup>I-MIBG planar imaging and SPECT/CT.

**Key Words:** neuroblastoma; <sup>124</sup>I; <sup>124</sup>I-MIBG; metaiodobenzylguanidine; PET/CT

**J Nucl Med 2021; 62:43–47**

DOI: 10.2967/jnumed.120.243139

---

**N**euroblastoma is the most common cancer in children less than 1 y old and accounts for approximately 6%–8% of all cancers in children (1). Approximately 90% of neuroblastoma cases are diagnosed before the age of 5 y. Neuroblastoma develops along the sympathetic nervous system, with approximately 80% of the tumors occurring in the abdomen (2). Metastatic disease is found in about half the cases at the time of diagnosis, with the most frequent sites of metastatic disease being bone and bone marrow (involving osseous structures from the skull and spine to the appendicular skeleton), followed by liver and skin (3). Several factors are involved in staging and risk classification for neuroblastoma, as recently defined by the system of the International Neuroblastoma Risk Group (4). Initial assessment of tumor extent uses this system's stage of L1 (localized tumor without image-defined risk factors for surgery), L2 (locoregional tumor with image-defined risk factors), and M (metastatic) or MS (metastatic in infant < 18 mo old with metastases limited to liver, skin, and bone marrow) (5). Other clinical and biologic risk factors include age, MYCN gene status, tumor cell histology, and ploidy. On the basis of this staging system, <sup>123</sup>I-metaiodobenzylguanidine (MIBG) planar scintigraphy is recommended before tumor excision during diagnosis of neuroblastoma and during follow-up after treatment for monitoring the extent of the tumor and its response to therapy (3,6). Previous studies showed that assessment of metastatic disease is better with <sup>123</sup>I SPECT/CT than with planar <sup>123</sup>I-MIBG imaging because of improved anatomic localization and improved lesion contrast in the SPECT/CT (7,8).

<sup>124</sup>I is a positron-emitting radionuclide that has a 4.2-d half-life, making it attractive for delayed clinical imaging and dosimetry. <sup>124</sup>I-MIBG PET has been used for imaging of malignant pheochromocytoma, demonstrating improved tumor delineation due to higher-resolution images than are obtainable with <sup>123</sup>I-MIBG SPECT (9). We have previously shown that <sup>124</sup>I-MIBG PET/CT can be used in children with neuroblastoma for accurate tumor dosimetry before <sup>131</sup>I-MIBG therapy (10,11).

In our study, we performed PET/CT imaging studies using no-carrier-added <sup>124</sup>I-MIBG, which is particularly important since it

---

Received Feb. 17, 2020; revision accepted Apr. 16, 2020.

For correspondence or reprints contact: Youngho Seo, UCSF Physics Research Laboratory, Department of Radiology and Biomedical Imaging, University of California, San Francisco, CA 94143.

E-mail: youngho.seo@ucsf.edu

<sup>†</sup>Deceased.

Published online May 15, 2020.

COPYRIGHT © 2021 by the Society of Nuclear Medicine and Molecular Imaging.

is a direct match to a recently approved no-carrier-added  $^{131}\text{I}$ -MIBG (Azedra; Progenics Pharmaceuticals). Here, we report the results of first-in-humans imaging studies in patients with neuroblastoma.

## MATERIALS AND METHODS

### Subjects

Patients were eligible if they had relapsed or refractory high-risk neuroblastoma, with confirmation of the diagnosis by histologic verification of the tumor, or if they had typical infiltration of tumor cells in bone marrow with elevated urinary catecholamine levels. They also were required to be at least 3 y old, and they or their parents or guardians had to have provided written informed consent for the  $^{131}\text{I}$ -MIBG treatment. Patients who required general anesthesia for MIBG imaging studies were excluded. The study was approved by our institutional review board.

### Imaging

No-carrier-added  $^{124}\text{I}$ -MIBG was either synthesized at our institution, using resins provided by our industry collaborator (Progenics Pharmaceuticals), or purchased from a commercial radiopharmacy (3D Imaging) under investigational-new-drug application 113907. No difficulties were encountered in the supply of  $^{124}\text{I}$ -MIBG or in the quality assurance steps during our study.  $^{124}\text{I}$ -MIBG PET/CT scans were obtained on a Discovery VCT PET/CT camera (GE Healthcare) for 6 patients and a Gemini TF PET/CT camera (Philips Healthcare) for 2 patients. There were no significant differences that could impact clinical interpretation between the PET scans obtained on the Discovery VCT and those obtained on the Gemini TF. This imaging study was performed in parallel with a pretherapy dosimetry study for 5 patients; therefore, these 5 patients, who were imaged before MIBG therapy, had multiple imaging time points, with the 24-h scan being used for image interpretation, whereas the posttherapy scan was a single scan at 24 h after  $^{124}\text{I}$ -MIBG administration. For those who did not complete imaging at multiple time points for the pretherapy dosimetry study, only the 24-h imaging time point was captured after  $^{124}\text{I}$ -MIBG administration. Because of the low activity of the administered  $^{124}\text{I}$ -MIBG, PET data were acquired for at least 4 min per bed position.  $^{123}\text{I}$ -MIBG imaging using whole-body planar imaging as well as focused-field-of-view SPECT/CT was performed on all patients 24 h after administration of a 5.2 MBq/kg dose of the radiotracer. The studies were performed between 2013 and 2017. Lesion locations, total numbers of lesions, and curie scores (3) were recorded using 2 independent interpretations by 2 nuclear medicine physicians. The curie score was calculated per the standard method described below for  $^{123}\text{I}$ -MIBG and  $^{131}\text{I}$ -MIBG planar scans. For  $^{124}\text{I}$ -MIBG PET, the curie score was calculated using the maximum-intensity-projection images. The planar, SPECT, and PET/CT scans that were compared in terms of lesion number and curie score were performed within 1 mo of each other. All positive lesions were confirmed on cross-sectional imaging. The scoring was based on division of the body into 9 anatomic sectors for osseous lesions (skull, upper arms, lower arms, chest, upper spine, lower spine, pelvis, upper legs, and lower legs) and a separate section for any extraosseous metastases, as described by Matthay et al. (12). In each of the regions, the lesions were scored as 0 for no lesion within the segment, 1 for 1 lesion within the segment, 2 for more than 1 lesion in the segment, and 3 for greater than 50% involvement of the segment. The absolute score was obtained by adding the scores of all the segments. There was a high concordance rate between the 2 reads, with the Fleiss  $\kappa$  measuring 0.783 (confidence interval, 0.6417–0.9702). If there was any discrepancy between the readers, the higher value was used for the study.

### Radiation Dosimetry of $^{124}\text{I}$ -MIBG

For the 5 patients who completed the  $^{124}\text{I}$ -MIBG dosimetry scans, we performed a full dose estimation, particularly for effective dose. For the dosimetry of  $^{124}\text{I}$ -MIBG, PET imaging was performed within

the first 4 h after injection and at 24, 48, and 120 h. The general method for our dose calculation was described previously (10). For the current study, one improved technique using patient-specific CT as a voxelized phantom for Monte Carlo simulation was used over what was reported before. From organ doses calculated from the Monte Carlo simulation—combined with time-integrated activity coefficients, also known as residence times, derived from 3 or 4 PET/CT images—International Commission on Radiological Protection publication 103 weighting factors were applied, and effective doses for each patient were calculated.

### Statistical Analysis

Continuous-variable data were analyzed across pretreatment and posttreatment scans using 2-sample *t* tests. Categorical variable data were analyzed with the  $\chi^2$  test. Statistical analysis was performed on STATA (StataCorp).

## RESULTS

In our study, 5 of the enrolled patients also underwent  $^{131}\text{I}$ -MIBG therapy for widely metastatic neuroblastoma, and 8 patients underwent the paired imaging with standard whole-body planar and focused-field-of-view  $^{123}\text{I}$ -MIBG SPECT/CT. In the 5 patients who received therapy, pretherapy whole-body  $^{124}\text{I}$ -MIBG PET/CT was performed, and in 2 patients, both pretherapy and follow-up posttherapy  $^{124}\text{I}$ -MIBG PET/CT was performed. The mean age of the patients was 11.6 y, with a range of 6–23 y.

### Detection of Lesions Using $^{124}\text{I}$ -MIBG PET/CT Versus $^{123}\text{I}$ -MIBG Scans

$^{123}\text{I}$ -MIBG whole-body planar scans, focused-field-of-view SPECT/CT scans, and whole-body  $^{124}\text{I}$ -MIBG PET scans found 25, 32, and 87 lesions, respectively, in 10 sets of matched scan data (Fig. 1). All but 1 (i.e., 24) of the lesions detected on  $^{123}\text{I}$ -MIBG planar imaging were clearly detected on  $^{124}\text{I}$ -MIBG PET/CT. The single lesion that was not detected by  $^{124}\text{I}$ -MIBG PET/CT was in the thoracic spine. Evaluation of  $^{124}\text{I}$ -MIBG uptake within the thoracic spine for this patient was limited by significant motion of the patient during that section of the scan and by background uptake, which affected detection of this lesion. However, 62 lesions that were detected on  $^{124}\text{I}$ -MIBG PET/CT were not detected on  $^{123}\text{I}$ -MIBG planar imaging, and 55 lesions that were detected on  $^{124}\text{I}$ -MIBG PET/CT were not detected on  $^{123}\text{I}$ -MIBG SPECT/CT (Fig. 1A). Detection of individual lesions on  $^{124}\text{I}$ -MIBG PET/CT differed to a statistically significant extent from that on  $^{123}\text{I}$ -MIBG planar imaging ( $P < 0.0001$ ) and  $^{123}\text{I}$ -MIBG SPECT/CT ( $P < 0.0001$ ).

### Lesion Detection and Curie Scores for $^{124}\text{I}$ -MIBG PET

Ten  $^{124}\text{I}$ -MIBG PET scans were obtained within 2 wk of  $^{123}\text{I}$ -MIBG planar imaging scans. Curie scores were obtained by a masked review by 2 nuclear medicine physicians with expertise in pediatric imaging. Of the 10 scans, 6 had higher curie scores than on the  $^{123}\text{I}$ -MIBG planar imaging scans and 4 had higher curie scores than on the  $^{123}\text{I}$ -MIBG planar and SPECT/CT combined interpretation (Fig. 1B).

### Localization of Lesions Based on the Part of the Body

Cross-sectional imaging provides an advantage in localizing lesions with complex 3-dimensional structures. In our patient cohort,  $^{124}\text{I}$ -MIBG PET/CT was more sensitive in detecting lesions within the chest, with the chest component of the curie score being higher than on planar imaging for 4 patients and higher than on SPECT/CT for 3 patients. Regarding the head and neck, 2 patients had higher head components of the curie scores than on planar imaging and 1 patient had higher scores than on SPECT/CT (Fig. 2

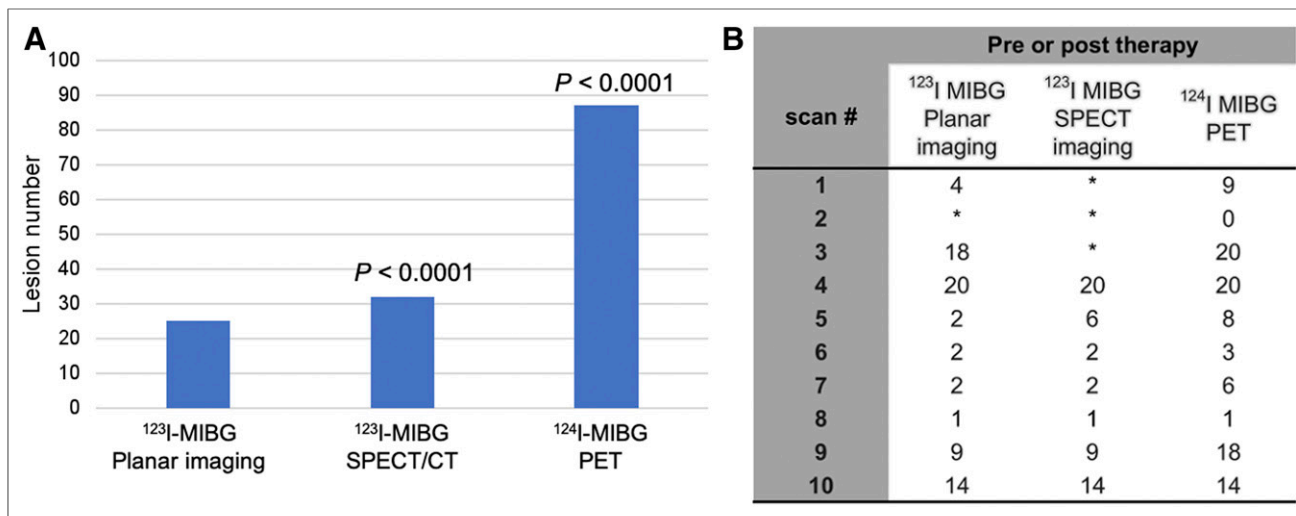


**FIGURE 1.** (A) Number of lesions on <sup>123</sup>I-MIBG planar and SPECT/CT scans was compared with number of lesions on <sup>124</sup>I-MIBG PET scans, among all 8 patients, and the difference was found to be statistically significant. (B) Curie score comparison between <sup>123</sup>I-MIBG planar, SPECT/CT, and <sup>124</sup>I-MIBG PET scans demonstrated higher overall curie scores on PET imaging for 6 scans.

and Supplemental Tables 1–8; supplemental materials are available at <http://jnm.snmjournals.org>). Another region of high discrepancy between the planar imaging read and the PET/CT read was the thoracic and lumbar spine. Regarding the thoracic spine, 4 patients had a higher component score on PET/CT than on <sup>123</sup>I planar imaging, and 2 patients had a higher component score on PET/CT than on SPECT/CT. These results suggest that <sup>124</sup>I-MIBG PET/CT is better at detecting lesions within the chest, spine, and head and neck than SPECT/CT—regions that are traditionally evaluated with SPECT/CT for more accurate lesion detection than can be obtained with planar imaging.

#### Radiation Exposure from Low-Dose <sup>124</sup>I-MIBG PET/CT Compared with <sup>123</sup>I-MIBG Planar Imaging and SPECT/CT

There is a significant difference in half-lives between <sup>124</sup>I and <sup>123</sup>I, with the former being 100 h and the latter being 13.2 h. This difference can potentially result in a higher effective dose for patients undergoing <sup>124</sup>I-MIBG. In our study, the estimated effective doses were 0.161 mSv/MBq for a 122-kg female, 0.235 mSv/MBq for a 63-kg male, 0.339 mSv/MBq for a 40-kg male, 0.706 mSv/MBq for a 29-kg female, and 0.795 mSv/MBq for a 23-kg female. These effective doses agreed well with our estimated effective doses for human subjects extrapolated from the data obtained in murine models (13). The previously estimated effective doses, using International Commission on Radiological Protection publication 103 weighting factors, were 0.252 mSv/MBq for a 73.7-kg male, 0.342 mSv/MBq for a 57-kg female, 0.388 mSv/MBq for a 56.8-kg 15-y-old, 0.578 mSv/MBq for a 33.2-kg 10-y-old, and 1.027 mSv/MBq for a 19.8-kg 5-y-old. These values are approximately 10 times higher than those of <sup>123</sup>I-MIBG (0.019 mSv/MBq for a 73.7-kg male). However, the effective dose for <sup>124</sup>I-MIBG imaging (1.05 MBq/kg administered) was only approximately twice the dose for <sup>123</sup>I-MIBG imaging (5.2 MBq/kg administered) because of the low-administered-dose protocol.

#### DISCUSSION

Accurate detection of metastatic disease is critical in high-risk neuroblastoma because semiquantitative MIBG scoring has been shown to correlate with patient outcomes at diagnosis (12) and

during treatment (14,15). The curie score has been developed for planar <sup>123</sup>I-MIBG scans for detection and quantitation of metastatic disease (16) but may be prone to an interpretation bias when there is faint uptake or difficulty in identifying disease within anatomically complex regions of the head and neck, spine, chest, and pelvis. To circumvent this limitation, many institutions perform limited SPECT/CT of the abdomen and pelvis to improve detection of disease, with modification of the curie score to reflect findings on planar and SPECT/CT images. Whole-body SPECT/CT is not routinely performed in clinical practice because of the length of examination, which can take more than an hour. On the other hand, whole-body PET/CT can be performed within 40 min even with a low-dose protocol similar to that used in our study and can provide a single, unified, semiquantitative score for patient metastatic status.

To the best of our knowledge, our study was the first-in-humans imaging study of metastatic neuroblastoma with <sup>124</sup>I-MIBG PET/CT. We demonstrated that <sup>124</sup>I-MIBG PET/CT is better able to detect tumors than <sup>123</sup>I-MIBG planar imaging and SPECT/CT. The increased detection of tumors also translated to higher curie scores in patients, as interpreted by 2 board-certified nuclear medicine physicians. The lesions that were better detected on <sup>124</sup>I-MIBG PET were predominantly within the chest, spine, head and neck, and upper and lower extremities. The long half-life of <sup>124</sup>I-MIBG allowed subsequent imaging of patients over the course of 3 d, thus enabling quantitative assessment of <sup>124</sup>I-MIBG dynamic binding and better prediction of dosimetry, in addition to diagnostic-quality imaging. The effective dose to the patients in our study was only twice that of the <sup>123</sup>I-MIBG scan; therefore, this tracer could be considered a safe alternative for patients with metastatic neuroblastoma.

One limitation of our study was the small number of patients, as may have been due to the fact that most children with neuroblastoma are young and would require anesthesia for these additional studies. We had 10 <sup>124</sup>I-MIBG PET scans performed on 8 patients during different time points of their <sup>131</sup>I-MIBG therapy, with most being imaged before treatment. Because few patients consented to the follow-up <sup>124</sup>I-MIBG PET/CT scan, information is lacking on evaluation of response and correlation with progression-free survival. Now that we have established the much greater sensitivity for

## <sup>123</sup>I-MIBG Planar Imaging

## <sup>124</sup>I-MIBG PET Imaging

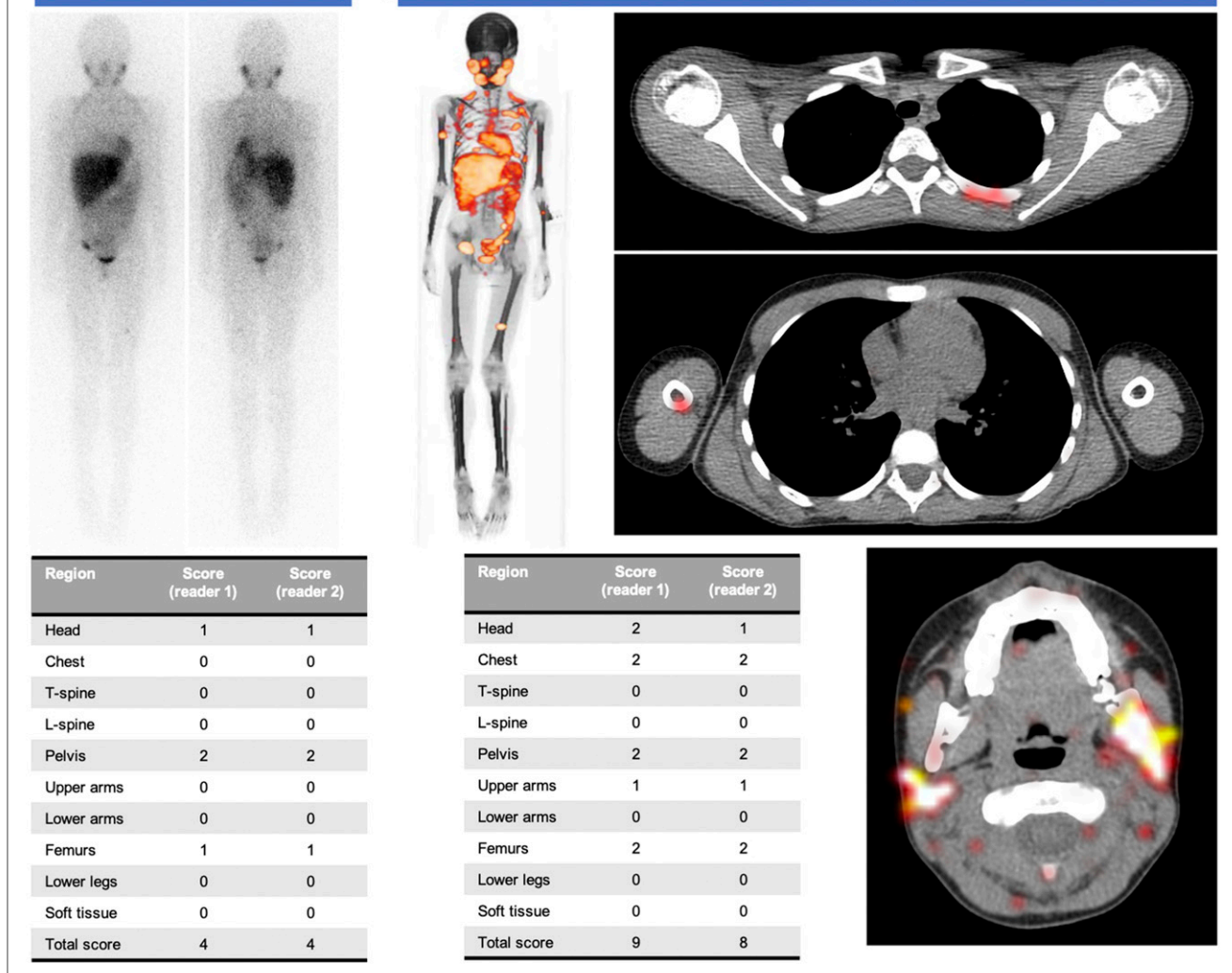


**FIGURE 2.** Planar anterior (left) and posterior (right) <sup>123</sup>I-MIBG planar images are compared with <sup>124</sup>I-MIBG PET/CT 3-dimensional volume-rendered and cross-sectional superimposed images of same patient. Lesions within chest, extremities, spine, and head and neck were better detected on planar images. Lesions within chest, upper arms, and head were better detected on PET/CT images.

detection of metastatic disease than is obtainable with standard <sup>123</sup>I-MIBG, further research on this radiotracer in a larger number of patients is indicated, without the need for concomitant <sup>123</sup>I-MIBG scans. Also, for patients who underwent both serial <sup>124</sup>I-MIBG imaging and <sup>131</sup>I-MIBG therapies, we did not have serial <sup>131</sup>I-MIBG scan data from which to calculate the absorbed dose from <sup>131</sup>I-MIBG therapy and to compare <sup>131</sup>I-MIBG doses with predicted doses from <sup>124</sup>I-MIBG scans. Although we had limited data to compare predicted lesion doses with therapy response for these patients, the number of patients was too small to claim any statistical significance at this point. Further research into detection of neuroblastoma with low uptake of MIBG-based tracers (i.e., <sup>123</sup>I-MIBG and <sup>124</sup>I-MIBG) and comparison to <sup>18</sup>F-FDG PET will also be needed to establish the role that <sup>124</sup>I-MIBG PET will play in clinical management of patients. Such research will establish the role of improved detection of metastatic disease in diagnosis and monitoring of metastatic neuroblastoma. The effective dose calculated for <sup>124</sup>I-MIBG in our cohort was in the range of 0.161–0.795

mSv/MBq, which is approximately 10–20 times the effective dose of <sup>18</sup>F-FDG in the pediatric population (17). For this reason, we chose to inject a very low activity (1.05 MBq/kg) with the trade-off of imaging for a longer time and having noisy images overall. Hence, we propose that <sup>124</sup>I-MIBG PET/CT may play an important role in follow-up imaging of patients, and further investigation into the negative predictive value of this test for patient outcomes is under way.

### CONCLUSION

The first-in-humans use of low-dose <sup>124</sup>I-MIBG PET for monitoring disease burden demonstrated tumor detection capability superior to that of <sup>123</sup>I-MIBG planar imaging and SPECT/CT.

### DISCLOSURE

This work was supported in part by the National Cancer Institute under grants R01 CA154561 and P01 CA081403 and by the Alex

Scott Lemonade Stand Foundation and the Dougherty Foundation. No other potential conflict of interest relevant to this article was reported.

## ACKNOWLEDGMENTS

We thank the clinical coordinators, cyclotron team, technologists, nurses, and physicians who made this study possible at the University of California, San Francisco. We also appreciate Progenics Pharmaceuticals for sharing the resins for  $^{124}\text{I}$ -MIBG for our initial human studies. We are particularly grateful to the late Dr. Randall Hawkins and Xiao Wu, who made significant contributions to the present study.

## KEY POINTS

**QUESTION:** Is low-dose no-carrier-added  $^{124}\text{I}$ -MIBG PET/CT superior to  $^{123}\text{I}$ -MIBG planar and SPECT/CT imaging for monitoring disease burden in patients with relapsed neuroblastoma?

**PERTINENT FINDINGS:** At a low effective dose (~2 times that of  $^{123}\text{I}$ -MIBG),  $^{124}\text{I}$ -MIBG PET/CT scans showed a statistically significant superior detection of lesions when compared with  $^{123}\text{I}$ -MIBG planar and SPECT/CT scans. The curie scores were also higher with  $^{124}\text{I}$ -MIBG PET/CT in 6 of 10 scans evaluated in the study.

**IMPLICATIONS FOR PATIENT CARE:**  $^{124}\text{I}$ -MIBG PET/CT may replace currently performed  $^{123}\text{I}$ -MIBG planar imaging and SPECT/CT in monitoring disease burden in patients with relapsed neuroblastoma.

## REFERENCES

- Berthold F, Spix C, Kaatsch P, Lampert F. Incidence, survival, and treatment of localized and metastatic neuroblastoma in Germany 1979-2015. *Paediatr Drugs*. 2017;19:577-593.
- Brisse HJ, McCarville MB, Granata C, et al. Guidelines for imaging and staging of neuroblastic tumors: consensus report from the International Neuroblastoma Risk Group Project. *Radiology*. 2011;261:243-257.
- Bar-Sever Z, Biassoni L, Shulkin B, et al. Guidelines on nuclear medicine imaging in neuroblastoma. *Eur J Nucl Med Mol Imaging*. 2018;45:2009-2024.
- Parikh NS, Howard SC, Chantada G, et al. SIOP-PODC adapted risk stratification and treatment guidelines: recommendations for neuroblastoma in low- and middle-income settings. *Pediatr Blood Cancer*. 2015;62:1305-1316.
- Matthay KK, Shulkin B, Ladenstein R, et al. Criteria for evaluation of disease extent by  $^{123}\text{I}$ -metaiodobenzylguanidine scans in neuroblastoma: a report for the International Neuroblastoma Risk Group (INRG) Task Force. *Br J Cancer*. 2010;102:1319-1326.
- Uehara S, Yoneda A, Oue T, et al. Role of surgery in delayed local treatment for INSS 4 neuroblastoma. *Pediatr Int*. 2017;59:986-990.
- Rozovsky K, Koplewitz BZ, Krausz Y, et al. Added value of SPECT/CT for correlation of MIBG scintigraphy and diagnostic CT in neuroblastoma and pheochromocytoma. *AJR*. 2008;190:1085-1090.
- Rufini V, Fisher GA, Shulkin BL, Sisson JC, Shapiro B. Iodine-123-MIBG imaging of neuroblastoma: utility of SPECT and delayed imaging. *J Nucl Med*. 1996;37:1464-1468.
- Hartung-Knemeyer V, Rosenbaum-Krumme S, Buchbender C, et al. Malignant pheochromocytoma imaging with [ $^{124}\text{I}$ ]mIBG PET/MR. *J Clin Endocrinol Metab*. 2012;97:3833-3834.
- Huang SY, Bolch WE, Lee C, et al. Patient-specific dosimetry using pretherapy [ $^{124}\text{I}$ ]m-iodobenzylguanidine ([ $^{124}\text{I}$ ]mIBG) dynamic PET/CT imaging before [ $^{131}\text{I}$ ]mIBG targeted radionuclide therapy for neuroblastoma. *Mol Imaging Biol*. 2015;17:284-294.
- Seo Y, Gustafson WC, Dannoon SF, et al. Tumor dosimetry using [ $^{124}\text{I}$ ]m-iodobenzylguanidine microPET/CT for [ $^{131}\text{I}$ ]m-iodobenzylguanidine treatment of neuroblastoma in a murine xenograft model. *Mol Imaging Biol*. 2012;14:735-742.
- Matthay KK, Edeline V, Lumbroso J, et al. Correlation of early metastatic response by  $^{123}\text{I}$ -metaiodobenzylguanidine scintigraphy with overall response and event-free survival in stage IV neuroblastoma. *J Clin Oncol*. 2003;21:2486-2491.
- Lee CL, Wahnische H, Sayre GA, et al. Radiation dose estimation using pre-clinical imaging with  $^{124}\text{I}$ -metaiodobenzylguanidine (MIBG) PET. *Med Phys*. 2010;37:4861-4867.
- Kushner BH, Yeh SD, Kramer K, Larson SM, Cheung NK. Impact of metaiodobenzylguanidine scintigraphy on assessing response of high-risk neuroblastoma to dose-intensive induction chemotherapy. *J Clin Oncol*. 2003;21:1082-1086.
- Yanik GA, Parisi MT, Naranjo A, et al. Validation of postinduction curie scores in high-risk neuroblastoma: a children's oncology group and SIOPEN group report on SIOPEN/HR-NBL1. *J Nucl Med*. 2018;59:502-508.
- Sharp SE, Trout AT, Weiss BD, Gelfand MJ. MIBG in neuroblastoma diagnostic imaging and therapy. *Radiographics*. 2016;36:258-278.
- Quinn BM, Gao Y, Mahmood U, et al. Patient-adapted organ absorbed dose and effective dose estimates in pediatric  $^{18}\text{F}$ -FDG positron emission tomography/computed tomography studies. *BMC Med Imaging*. 2020;20:9.